Bronchioalveolar Stem Cells Derived from Mouse Induced Pluripotent Stem Cells Promote Airway Epithelium Regeneration

Naoya Kawakita
Tokushima Daigaku Igakubu Daigakuin Ikgaku Kyoikubu https://orcid.org/0000-0001-9288-7478
Hiroaki Toba (ht1109@tokushima-u.ac.jp)
Keiko Miyoshi
Tokushima Daigaku Daigakuin Ishiyakugaku Kenkyubu
Shinichi Sakamoto
Tokushima Daigaku Igakubu Daigakuin Ikgaku Kyoikubu
Daisuke Matsumoto
Tokushima Daigaku Igakubu Daigakuin Ikgaku Kyoikubu
Mika Takashima
Tokushima Daigaku Igakubu Daigakuin Ikgaku Kyoikubu
Mariko Aoyama
Tokushima Daigaku Igakubu Daigakuin Ikgaku Kyoikubu
Seiya Inoue
Tokushima Daigaku Igakubu Daigakuin Ikgaku Kyoikubu
Masami Morimoto
Kyoto Daini Sekijuji Byoin
Takeshi Nishino
Tokushima Daigaku Igakubu Daigakuin Ikgaku Kyoikubu
Hiromitsu Takizawa
Tokushima Daigaku Igakubu Daigakuin Ikgaku Kyoikubu
Akira Tangoku
Tokushima Daigaku Igakubu Daigakuin Ikgaku Kyoikubu

Research

Keywords: induced pluripotent stem cells, stem cell transplantation, progenitor cells, tissue regeneration

Posted Date: July 8th, 2020

DOI: https://doi.org/10.21203/rs.3.rs-40560/v1

Version of Record: A version of this preprint was published on October 2nd, 2020. See the published version at https://doi.org/10.1186/s13287-020-01946-7.

Abstract

Background: Bronchioalveolar stem cells (BASCs) located at the bronchioalveolar-duct junction (BADJ) are stem cells residing in alveoli and terminal bronchioles that can self-renew and differentiate into alveolar type (AT)-1 cells, AT-2 cells, club cells, and ciliated cells. Following terminal-bronchiole injury, BASCs increase in number and promote repair. However, whether BASCs can be differentiated from mouse-induced pluripotent stem cells (iPSCs) remains unreported, and the therapeutic potential of such cells is unclear. We sought to differentiate BASCs from iPSCs and examine their potential for use in the treatment of epithelial injury in terminal bronchioles.

Methods: BASCs were induced using a modified protocol for differentiating mouse iPSCs into AT-2 cells. Differentiated iPSCs were intratracheally transplanted into naphthalene-treated mice. The engrafted BASCs on BADJ, and its ability to promote repair an injury to the airway epithelium, were evaluated.

Results: Flow cytometric analysis revealed that BASCs represented ~7% of the cells obtained. Additionally, ultrastructural analysis of these iPSC-derived BASCs by using transmission electron microscopy showed that the cells containing secretory granules harboured microvilli and small and immature lamellar body-like structures. When the differentiated iPSCs were intratracheally transplanted in naphthalene-induced airway epithelium injury, transplanted BASCs were found to be engrafted in the BADJ epithelium and alveolar spaces for 14 d after transplantation and to maintain the BASC phenotype. Notably, repair of the terminal-bronchiole epithelium was markedly promoted after transplantation of the differentiated iPSCs.

Conclusions: Mouse iPSCs could be differentiated *in vitro* into cells that display a similar phenotype to BASCs. Notably, the differentiated iPSCs promoted airway epithelium at the BADJ in the mouse model of naphthalene-induced airway epithelium injury.

Background

The lung features a complex internal structure that harbours multiple epithelial cell types, including bronchial and alveolar epithelial cells, and pulmonary endothelial cells. The lung epithelium plays specialized roles in respiration and host defence, and lung epithelial cells can be repaired following damage by infection, air pollutants, and various irritants; this repair of the lung and bronchiole epithelium is governed by stem cell populations present in distinct niches along the proximal–distal axis [1, 2]. Interaction between lung stem cells and their niche is critical for maintaining the balance between stem cells and differentiated cells, and an imbalance between these cell populations causes inappropriate repair and leads to the development of lung diseases such as chronic obstructive pulmonary disease, idiopathic pulmonary fibrosis, and lung cancer [3].

In terminal bronchioles in the mouse lung, the percentage of club cells among epithelial cells is known to be high (~ 90%) [4], and a widely recognized club cell-specific cytotoxicant is naphthalene; therefore, the mouse model of naphthalene-induced peripheral airway injury is frequently used in regeneration studies

[5–12]. After club cell depletion, the residual cells in the terminal bronchioles can complete the repair of the epithelium and regenerate the cells appropriate for this lung region [11–13]. In this process, the stem cells that renew the terminal-bronchiole epithelium by proliferating and differentiating into club cells are called bronchioalveolar stem cells (BASCs) [2, 6, 10, 14–24].

BASCs that localize at the bronchioalveolar-duct junction (BADJ) and co-express markers of club cells and alveolar type (AT)-2 cells have recently been regarded as local stem cells used for lung repair. BASCs can self-renew and differentiate into club cells, AT-1 cells, AT-2 cells, and ciliated cells [22, 23, 25], and, notably, BASCs increase in number during the repair process in naphthalene-induced airway injury [6, 19]. Therefore, we hypothesized that BASC transplantation might promote repair in naphthalene-induced airway injury. BASCs can be isolated from adult mouse lungs by using flow cytometry, but a hurdle here is that the BASC population represents < 1% of the total lung cells [14, 26].

Induced pluripotent stem cells (iPSCs), which are obtained by introducing Yamanaka factors into differentiated somatic cells, display self-renewal properties and pluripotency [27]. AT-2 cells or lung progenitor cells have been derived from mouse iPSCs or embryonic stem cells (ESCs) in several studies either through embryoid body (EB) formation or by using differentiation medium, and the therapeutic potential of the iPSC-derived cells has also been reported [28–41]. However, no study thus far has reported the *in vitro* differentiation of iPSCs into BASCs, and the therapeutic potential of BASCs remains unclear. Here, we generated iPSC-derived BASCs and intratracheally transplanted these cells in a mouse model of naphthalene-induced airway injury to evaluate the therapeutic potential of these cells in the repair of damaged club cells.

Methods

Cell line and culture

A mouse iPSC line (iPS-MEF-Ng-492B-4) was purchased from the RIKEN Cell Bank (Tsukuba, Japan; http://www.brc.riken.go.jp/lab/cell) and maintained on a feeder layer of 3×10^4 cells/cm^2 mitomycin C-inactivated mouse SNL76/7 cells (European Cell Culture Collection, Porton Down, UK, EC07032801); mitomycin C was from Kyowa Kirin Co., Ltd. (Tokyo, Japan). The cells were cultured on 0.1% gelatin-coated tissue-culture dishes, in iPS medium containing KnockOut™ Dulbecco's modified Eagle's medium (DMEM; Gibco, Carlsbad, CA) supplemented with 15% KnockOut™ Serum Replacement (Gibco), 0.1 mM nonessential amino acids (Gibco), 0.1 mM 2-mercaptoethanol (Gibco), 1× GlutaMAX™-I (Gibco), and 1000 U/mL murine Leukemia Inhibitory Factor (Wako Pure Chemical Industries, Osaka, Japan) at 37°C in a humidified atmosphere of 5% CO_2. This iPSC line expresses green fluorescent protein (GFP) under the control of *Nanog* promoter.

iPSC differentiation

For inducing the differentiation of mouse iPSCs into BASCs, a previously reported method for inducing AT-2 cells was used [36]. Briefly, mouse iPSCs were harvested using TrypLE^{TM} Express Enzyme solution (Gibco) and incubated for 1 h on 0.1% gelatin-coated dishes. During this procedure, a majority of the feeder SNL cells contained in the cell suspension reattached to the bottom of the dishes. The supernatant containing the iPSCs was collected and the cell concentration was adjusted to 3×10^4/mL by using the differentiation medium mentioned below. To initiate EB formation, the hanging-drop method was used; 20-μL drops of the cell suspension in differentiation medium containing ~600 mixed cells were placed on the lid of bacteriological Petri dishes and incubated for 3 d, and EBs were then transferred to 96-well cell-repellent plates and cultivated for 2 d. After 5 d, EBs were plated onto 6-well culture dishes (10 EBs/well) coated with 0.1% gelatin and cultivated at until 24 d. The basal differentiation medium (BM) was composed of Iscove's modified Dulbecco's medium (Gibco), 0.2 mM L-glutamine (Gibco), 0.1 mM 2-mercaptoethanol, and 0.1 mM nonessential amino acids (Gibco). The BM was supplemented from 0 to 7 d with 15% fetal bovine serum (Gibco) and from 7 to 24 d with 15% KnockOut^{TM} Serum Replacement. The BM was further supplemented with the following growth factors: 20 ng/mL recombinant human keratinocyte growth factor (KGF; ProteinTech Inc., Tokyo, Japan) (from 0 to 24 d) and DCI (treatment protocol: □d10–d24 or □d14–d24); DCI is a three-factor combination of 10 nM dexamethasone (Sigma-Aldrich, St. Louis, MO) plus 0.1 mM 8-bromoadenosine 3´5´-cyclic monophosphate sodium salt (Sigma-Aldrich), and 0.1 mM 3-isobutyl-1-methylxanthine (Sigma-Aldrich). The medium was replaced every 2–3 d. The differentiation procedure is depicted schematically in Fig. 1a.

Animal care

Animals were housed in Micro-Isolator cages on a layer of wood shavings at a temperature of 22℃, under a fixed 12/12-h light/dark cycle. All studies were performed in accordance with the guidelines established by the Tokushima University committee on animal care and use. All experimental protocols were reviewed and approved by the animal research committee of the University of Tokushima, Japan.

Experimental design

Female C57/BL6 mice (8–12 weeks old) were used in all experiments. Mice in the Corn oil group were intraperitoneally treated with corn oil (Sigma-Aldrich) at a dose of 10 mL/kg body weight and then sacrificed 5 d after the treatment (n = 4). Mice in the naphthalene-treatment group (NA group), control group, and iPS group were intraperitoneally treated with naphthalene (Sigma-Aldrich) dissolved in corn oil at a dose 200 mg/kg body weight. On the day following the naphthalene treatment, the mice in the control and iPS groups were anesthetized using isoflurane inhalation, after which the control group mice received a single intratracheal injection of 50 μL of DMEM and the iPS group mice received a single intratracheal injection of differentiated iPSCs (1.0×10^6 cells/mouse, in 50 μL of DMEM). The transplanted cells were labelled using a PKH26 Red Fluorescent Cell Linker Mini Kit (Sigma-Aldrich), according to the manufacturer's protocol. The mice in each group were sacrificed at two time points: 5 d and 15 d (n = 4–6/group, at each time point).

Histological analysis

Differentiated iPSCs were dissociated into single-cell suspensions in PBS and centrifuged, and the pellets obtained were fixed with 10% formaldehyde for 1 h and then embedded in paraffin. The paraffin-embedded specimens were cut at 5 μm thickness for haematoxylin and eosin (H&E) staining or immunofluorescence analysis.

After mice were sacrificed, the lungs of the mice in the Corn oil group, NA group, and control group were harvested, and the left lung was fixed with 10% buffered formalin injected intratracheally and then used for histological studies; the remaining lung tissue was snap-frozen and stored at -80°C for RNA extraction. The lung tissues were embedded in paraffin and cut at 5-μm thickness, and the sections were stained with H&E or used for immunofluorescence analysis. The left lungs from mice in the iPS group were fixed (overnight, in the dark) using a mixture of 4% paraformaldehyde and optimal cutting temperature (OCT) compound (4:1) administered intratracheally; subsequently, these lungs were cut in half, and one half was frozen embedded in OCT compound and the other was embedded in paraffin. The frozen specimens were cut at 10 μm thickness for immunofluorescence analysis, and the paraffin-embedded specimens were cut at 5 μm thickness for H&E staining or immunofluorescence analysis.

Flow cytometry

To quantify BASCs among differentiated cells, flow cytometry was performed for (1) cytoplasmic markers and (2) surface markers. In the case of cytoplasmic markers, club-cell secretory protein (CCSP)-positive and surfactant protein C (SPC)-positive ($CCSP^{pos}/SPC^{pos}$) cells were quantified. Briefly, differentiated cells were dissociated into single-cell suspensions in PBS, and then IntraPrep permeabilization reagent (A07802; Beckman Coulter, Fullerton, CA) was used according to the manufacturer's protocol. The cells were stained for 15 min on ice with anti-mouse CCSP antibody conjugated with Alexa Fluor® 488 (1:100, sc-365992 AF488; Santa Cruz Biotechnology, Santa Cruz, CA) and anti-mouse SPC antibody conjugated with Alexa Fluor® 647 (1:100, bs-10067R-A647; Bioss Inc., Boston, MA). Flow cytometry was performed using a BD FACSVerse Flow Cytometer running BD FACSuite Software (BD Biosciences, San Jose, CA) and Kaluza Analysis Software (Beckman Coulter). In the case of surface markers, $Sca\text{-}1^{pos}/CD45.2^{neg}/CD31^{neg}$ cells were quantified according to previous reports [14, 26]. Single-cell suspensions of differentiated cells were stained for 15 min on ice with anti-mouse Sca-1 conjugated with FITC (1:100, #557405; BD Biosciences), anti-mouse CD45.2 conjugated with APC (1:100, #561875; BD Biosciences), and anti-mouse CD31 conjugated with APC (1:100, #561814; BD Biosciences). Flow cytometry was performed using a Cell Sorter LE-SH800S running SH800 software (SONY, Tokyo, Japan) and Kaluza Analysis Software.

Transmission electron microscopy (TEM)

From differentiated iPSCs, the $Sca\text{-}1^{pos}/CD45.2^{neg}/CD31^{neg}$ cell population was isolated using fluorescence-activated cell sorting (FACS). The sorted cells were fixed with 2% glutaraldehyde in 0.1 M phosphate buffer overnight at 4°C, washed in 0.1 M phosphate buffer, and post-fixed with 2% osmium

tetroxide in 0.1 M phosphate buffer for 2 h at 4℃. Next, the cells were dehydrated using a graded ethanol series, incubated in propylene oxide for 20 min, and impregnated by incubation in propylene oxide/epoxy resin (2:1 v/v) for 2 h and then propylene oxide/epoxy resin (1:1 v/v) overnight. On the following day, the samples were embedded in Epon812 (48 h at 60℃). Ultrathin sections (80 nm) were cut using an ultramicrotome, and for contrasting, the sections were incubated with 2% uranyl acetate for 15 min and lead citrate for 5 min. Lastly, the sections were imaged using an H-700 (HITACHI, Tokyo, Japan) transmission electron microscope operating at 100 kV.

Immunofluorescence

Undifferentiated iPSCs in 24-well plates were subject to live staining with mouse anti-mouse SSEA-1 antibody conjugated with DyLight™ 550 (StainAlive™ SSEA-1 Antibody, 09-00959; Stemgent, San Diego, CA). The cells in the wells were fixed with 4% paraformaldehyde in PBS for 20 min and blocked with 10% goat serum (PCN5000; Invitrogen, Carlsbad, CA) in PBS containing 0.1% Triton X-100 for 1 h at room temperature. After overnight incubation at 4°C with the primary antibody (1:100), rabbit anti-Sox2 (09-0024; Stemgent) or rabbit anti-Oct4 (09-0023; Stemgent), the wells were washed with PBS, and the cells were then exposed to the secondary antibody, anti-rabbit IgG conjugated with Alexa Fluor® 594 (1:100, A-11037; Invitrogen), for 1 h at room temperature. Lastly, the wells were washed with PBS and the cells were counterstained with DAPI (4´,6-diamidino-2-phenylindole dihydrochloride) (D3571; Invitrogen).

Paraffin-embedded sections were deparaffinized and antigens were retrieved using 2100 Antigen Retriever (Aptum Biologics Ltd.) containing 10 mM citric buffer (pH 6) at for 2.5 h. The sections were blocked with 5% BSA/PBS for 2 h at room temperature and then the following directly conjugated antibodies (1:100 in 5% BSA/PBS) were used for labelling: anti-mouse CCSP antibody conjugated with Alexa Fluor® 488 (sc-365992 AF488; Santa Cruz Biotechnology) and anti-mouse SPC antibody conjugated with Alexa Fluor® 647 (bs-10067R-A647; Bioss Inc.). After incubation with the antibodies for 1 h at room temperature in a humidified chamber, the sections were washed four times in PBS/0.3% Triton-X and mounted with ProLong™ Diamond Antifade Mountant containing DAPI (P36966; Invitrogen). Fluorescence images were captured using a fluorescence microscope (BZ-X800, Keyence; Osaka, Japan). CCSP-positive cells that were located within 200 μm of the BADJ and exhibited a specific nuclear labelling profile and clear attachment to the basement membrane were counted as club cells, from at least 5 BADJs [10].

Statistical analysis

All analyses were conducted using SPSS software (version 24, IBM Corp., Armonk, NY). All statistical tests were two-sided, and $P < 0.05$ was considered significant. All continuous values are expressed as means ± standard deviation (SD). Student's *t*-test was used to compare two groups of continuous variables. For comparing continuous variables of three or more groups, one-way ANOVA followed by Tukey's multiple-comparison test was used.

Results

Differentiation of iPSCs into BASCs

We maintained mouse iPSCs in culture and monitored their undifferentiated status until passage 25. Immunostaining for the mouse pluripotency markers SSEA-1, Nanog, Oct4, and Sox2 revealed that the iPSCs were positive for all four markers (See Supplementary Fig. S1, Additional File 1), which indicated that the iPSCs maintained their pluripotency. In this study, we used mouse iPSCs from passage 18 to passage 25. The results of FACS analysis at differentiation d24 showed that Sca-1^{pos}/$CD45.2^{neg}$/$CD31^{neg}$ cells, which included BASCs, constituted 15.1% ± 7.8% and 12.8% ± 7.9% of the cells in d10–d24 DCI and d14–d24 DCI groups, respectively. Moreover, the $CCSP^{pos}$/SPC^{pos} cell population, in which BASCs were further enriched, constituted 7.0% ± 5.3% and 4.9% ± 3.6% of the cells in d10–d24 DCI and d14–d24 DCI groups, respectively. The BASC ratio did not differ significantly between d10–d24 DCI and d14–d24 DCI groups (Fig. 1b). According to the labelling for both surface and intracellular markers, the ratio of BASCs in d10–d24 DCI group was slightly higher than that in d14–d24 DCI group, although the difference was not significant (surface markers: $P = 0.695$; cytoplasmic markers: $P = 0.604$). We used the protocol d10–d24 DCI for subsequent experiments. Immunofluorescence labelling of differentiated iPSCs also revealed the presence of a small number of $CCSP^{pos}$/SPC^{pos} cells (Fig. 1c).

Ultrastructure of differentiated iPSCs

To analyse the ultrastructure of iPSC-derived BASCs, the sorted Sca-1^{pos}/$CD45.2^{neg}$/$CD31^{neg}$ cells were examined using TEM. Club cells have been shown to contain a large number of secretory granules [42], and the presence of lamellar bodies and microvilli has been identified as a characteristic of both normal-lung AT-2 cells and ESC/iPSC-derived AT-2 cells [32, 36, 43]. Here, the sorted cells containing secretory granules harboured microvilli and small and immature lamellar body-like structure; the secretory granules varied in number depending on the cells, and the lamellar body-like structures were concentrated in the vesicles (Fig. 2).

Intratracheal transplantation of differentiated iPSCs into naphthalene-treated mice

To obtain a mouse distal airway injury model, naphthalene was intraperitoneally administered to female mice (Fig. 3a). Naphthalene, a club cell-specific cytotoxicant, was reported to cause particularly strong damage in female mice [11, 12, 44]. In our injury model, club cells were almost completely depleted on the second day after naphthalene treatment, but the cells were normally retained after the administration of corn oil (Fig. 3b).

We next labelled and quantified CCSP-positive cells at BADJs after different treatments (Fig. 4): At 5 d, the mean numbers of these cells in NA, control, iPS, and Corn oil groups were 5.3 ± 3.9, 5.2 ± 3.5, 8.1 ± 3.3, and 26.6 ± 3.5, respectively. The number of CCSP-positive cells was significantly increased in the Corn oil group ($P < 0.001$) but did not differ between the other groups (iPS group vs control group, $P = 0.198$; iPS group vs NA group, $P = 0.216$). At 15 d, the mean numbers of CCSP-positive cells at BADJs in NA, control, and iPS groups were 8.9 ± 3.3, 9.5 ± 5.6, and 13.3 ± 2.8, respectively. The recovery of CCSP-

positive club cells was significantly promoted in the iPS group (iPS group vs control group, $P = 0.013$; iPS group vs NA group, $P = 0.004$) (Fig. 4).

Engraftment of differentiated iPSCs

In mouse frozen lung sections, numerous PKH26-positive cells were detected in alveoli and terminal bronchioles at both 5 and 15 d, which verified the engraftment of transplanted differentiated iPSCs. The results of immunofluorescence labelling further demonstrated that these cells were $PKH^{pos}/CCSP^{pos}/SPC^{pos}$ and $PKH^{pos}/CCSP^{neg}/SPC^{neg}$, which confirmed the engraftment of the transplanted BASCs in mice at 5 d (Fig. 5). $PKH^{pos}/CCSP^{pos}/SPC^{pos}$ and $PKH^{pos}/CCSP^{pos}/SPC^{neg}$ cells were also similarly detected in mice at 15 d. Our results confirmed that the transplanted BASCs retained their stem cell characteristics for 2 weeks after transplantation and further that the engrafted $PKH^{pos}/CCSP^{pos}/SPC^{neg}$ cells were found to constitute the BADJ epithelium (Fig. 6).

Discussion

In this study, we showed that iPSC-derived BASCs transplanted into naphthalene-treated mice were engrafted in the lung and retained their BASC phenotype and, furthermore, promoted recovery from injury. Moreover, we revealed the ultrastructure of the iPSC-derived BASCs.

Naphthalene treatment in mice causes the selective shedding of terminal bronchiolar club cells, but this effect is reversible and recovery occurs spontaneously [12, 13]. Although the steady-state numbers of BASCs are very low, BASC numbers increase temporarily after naphthalene treatment and then return to pre-treatment levels; therefore, BASCs are considered to play critical roles as local stem cells during the repair of club cells [6, 19, 22]. We hypothesized that transplantation of exogenous BASCs, which would to add to the endogenous BASCs that are present, might result in reduced damage and promote repair. In adult mice, BASCs account for < 1% of the total lung cells, and thus a comparatively richer BASC population must be obtained for cell transplantation [14, 26]. Here, we successfully differentiated iPSCs into BASCs.

To differentiate iPSCs into BASCs, we used the protocol developed by Schmeckebier et al. for differentiating iPSCs into AT-2 cells [36]. To date, no study has reported ESC or iPSC differentiation into BASCs. However, because BASCs are recognized as progenitor cells of AT-2 cells, we suspected that BASCs could be obtained during the AT-2-cell differentiation process. From several protocols, we selected and applied the aforementioned protocol, which yielded cells in which CCSP mRNA levels were higher than in an AT-2 cell line [32, 36]. In the Schmeckebier et al. study, the mRNA levels of both CCSP and SPC were high in □d10–d24 DCI and □d14–d24 DCI in the presence of KGF [36]. Therefore, we compared the BASC-induction efficiency in the groups □d10–d24 DCI and □d14–d24 DCI, but found no statistically significant difference.

When BASCs were identified based on surface markers, $Sca\text{-}1^{pos}/CD45.2^{neg}/CD31^{neg}$ cells were found to constitute 15.1% ± 7.8% and 12.8% ± 7.9% of the cell populations in □d10–d24 DCI and □d14–d24 DCI

groups, respectively. Conversely, with identification based on cytoplasmic markers that define genuine BASCs, the $CCSP^{pos}/SPC^{pos}$ cell populations were found to be 7.0% ± 5.3% and 4.9% ± 3.6% in □d10–d24 DCI and □d14–d24 DCI groups. The ratio of the BASC-identification rate by surface markers to the rate by cytoplasmic markers was 46% and 38% in □d10–d24 DCI and □d14–d24 DCI groups, respectively. In a study conducted using total lung cells of adult mice, immunofluorescence labelling revealed that 85% of the $Sca\text{-}1^{pos}/CD45.2^{neg}/CD31^{neg}$ cell population co-expressed CCSP and SPC [14]. The percentage calculated in our study here was < 85%, and this disparity in the results might be due to the difference between cultured cells *in vitro* and total lung cells *in vivo*.

The $CCSP^{pos}/SPC^{pos}$ cell population, which represents BASCs, accounted for a small proportion of the cells (7.0% ± 5.3%) in □d10–d24 DCI group, and these cells were transplanted intratracheally. However, when the differentiated iPSCs were intratracheally transplanted into naphthalene-treated mice, more of the engrafted cells were $PKH^{pos}/CCSP^{pos}/SPC^{pos}$ cells and the number of $PKH^{pos}/CCSP^{neg}/SPC^{neg}$ cells was low (Figs. 5 and 6). Thus, cells displaying the BASC phenotype appeared to show increased likelihood of engraftment in naphthalene-treated mice. Moreover, this phenomenon was observed in mice not only at 5 d but also at 15 d. At 15 d, the transplanted BASCs were retained in the lung and the cells maintained the BASC phenotype ($PKH^{pos}/CCSP^{pos/}SPC^{pos}$).

To date, a few cell-therapy studies have been conducted using similar naphthalene-injury models [5, 7, 8]. Naphthalene treatment has been used not only for developing a model of airway injury that is to be ameliorated, but also as a “preconditioning regimen” to create an airway-specific niche for cell incorporation [7, 8]. When bone marrow cells or tissue stem cells were intratracheally transplanted into naphthalene-treated mice in previous studies, engraftment of CCSP-positive cells at the BADJ was observed [5, 8]. We focused here on BASCs, and our results demonstrated not only engraftment of the cells in the injury area, but also enhanced repair of the injury caused by naphthalene. This finding suggests that iPSC-derived BASCs could represent a favourable cell source in cell therapy.

At 5 d, the number of club cells was slightly higher in the iPS group than in the NA and control groups, but the difference was not significant. However, at 15 d, club cells at BADJs numbered 13.3 ± 2.8, 8.9 ± 3.3, and 9.5 ± 5.6 in the iPS, NA, and control groups, respectively, and markedly enhanced club cell repair was observed in the iPS group. At 15 d, engraftment of PKH26-positive BASCs ($PKH^{pos}/CCSP^{pos}/SPC^{pos}$) and PKH26-positive club cells ($PKH^{pos}/CCSP^{pos}/SPC^{neg}$) at the BADJ was observed. It remains unclear whether the engrafted BASCs transdifferentiated into club cells or whether the club cells contained in the transplanted cell population were engrafted. Considering that the administration of cell-derived exosomes was reported to promote the proliferation of endogenous BASCs [45], one possibility that exosomes from the transplanted iPSC-derived cells acted on endogenous cells to promote repair. Moreover, the pathway by which paracrine fibroblast growth factor 10 from parabronchial smooth muscle activates BASCs was reported to be critical for epithelial repair after naphthalene-induced injury [46]. Furthermore, the result obtained in genetic-lineage tracking of BASCs *in vivo* showed that not all of the repaired airway epithelium was derived from BASCs [22]. Therefore, the transplanted cell population containing BASCs

might engage in crosstalk with endogenous factors and cells and promote recovery from naphthalene-induced injury through direct cell repair or indirect effects.

Despite limitations associated with iPSC-derived cells, such as altered ultrastructure, we revealed the ultrastructure of BASCs for the first time here. BASCs have been studied from various genetic perspectives, but their ultrastructure has not been clarified [6, 14, 22, 23]. We found that iPSC-derived BASCs harboured immature lamellar body-like structures and microvilli characteristic of AT-2 cells and secretory granules characteristic of club cells. This finding is in accord with the BASCs showing the $CCSP^{pos}/SPC^{pos}$ phenotype in immunostaining.

To our knowledge, this study has shown for the first time that BASCs can be induced from mouse iPSCs. Moreover, our study confirmed not only that the iPSC-derived BASCs were engrafted in the mouse model of naphthalene-induced airway injury, but also that the BASCs promoted repair, which indicates that these cells can potentially be used for cell therapy. Although rapid progress has been made in deriving the lung epithelial lineage from ESCs and iPSCs, as reflected in our study, a major challenge that remains is the generation of complex 3D tissue structures, or even functional organs, from these cells. The functional structures that have been previously obtained by culturing cells in a monolayer, such as the retina or myocardial sheets, have been readily used in clinical applications [47, 48]. Recently, the regeneration of functional lungs has been challenged by using decellularized lungs as a 3D scaffold and then re-cellularising them [49, 50]. However, it has not yet been possible to replace the organ itself and maintain the function for an extended period, and the methodology required for delivering and retaining lung stem cell-based regenerative therapies to the injured lung remains under development. The transplantation of iPSC-derived progenitor cells, stromal cells isolated from human bone marrow, adipose tissue, and mesenchymal stromal cells to treat terminal-bronchiole/alveolar-region disorders (e.g., chronic obstructive pulmonary disease, bronchiolitis obliterans, acute lung injury) is expected to attenuate injury or promote regeneration [5, 32, 51–56]. The findings obtained using our cell-therapy method involving BASCs will also contribute to the further development of treatments for terminal-bronchiole/alveolar-region disorders.

Two limitations of this study are the following. First, all iPSC-derived differentiated cells were intratracheally transplanted, and we have not yet demonstrated that BASCs, representing only 7.0% ± 5.3% of the cells, contributed to the enhancement of repair. Because the BASCs required for transplantation cannot be readily obtained given the current induction efficiency, it will be necessary to further improve this efficiency and transplant isolated BASCs. However, the induction efficiency of AT-2 cells was reported to be 9–18%, and thus it might be challenging to markedly increase the induction efficiency of BASCs [28, 32, 33]. Second, the observation period after cell transplantation was 2 weeks, and the long-term dynamics of the engrafted BASCs remain unknown. Thus, it will be necessary to devise a cell-tracking method and perform long-term BASC tracking.

Conclusions

We demonstrated that mouse iPSCs could be differentiated *in vitro* into cells exhibiting the BASC phenotype. Notably, the differentiated iPSCs promoted club cell repair at the BADJ in the mouse model of naphthalene-induced airway epithelium injury.

Abbreviations

AT-1
Alveolar type-1; AT-2:Alveolar type-2; BASC:Bronchioalveolar stem cells; BADJ:Bronchioalveolar-duct junction; iPSC:Induced pluripotent stem cell; ESC:Embryonic stem cell; EB:embryoid body; DMEM:Dulbecco's modified Eagle's medium; OCT:Optimal cutting temperature; CCSP:Club-cell secretory protein; SPC:surfactant protein C; TEM:Transmission electron microscopy; FACS:Fluorescence-activated cell sorting; DAPI:4´,6-diamidino-2-phenylindole dihydrochloride; SD:Standard deviation.

Declarations

Ethics approval and consent to participate

All studies were performed in accordance with the guidelines established by the Tokushima University committee on animal care and use. All experimental protocols were reviewed and approved by the animal research committee of the University of Tokushima, Japan.

Consent for publication

Not applicable.

Availability of data and materials

Not applicable.

Competing interests

The authors declare that they have no competing interests.

Funding

This work was supported by Japan Society for the Promotion of Science from the KAKENHI (Grants-in-Aid for Scientific Research) (Grant Number JP15K10260).

Authors' contributions

NK collected and assembled the data, performed data analysis and interpretation, and was a contributor in writing the manuscript. HT conceived and designed experiments, acquired financial support, performed data analysis and interpretation, and gave final approval of manuscript. SS provided study materials. KM provided administrative support. DM performed data analysis and interpretation. MT provided study

materials. MA provided study materials. SI performed data analysis and interpretation. MM acquired financial support. TN acquired financial support. HT provided administrative support. AT provided administrative support

Acknowledgments

This work was supported by the Support Center for Advanced Medical Sciences, Tokushima University Graduate School of Biomedical Sciences.

References

1. Rock JR, Onaitis MW, Rawlins EL, Lu Y, Clark CP, Xue Y, et al. Basal cells as stem cells of the mouse trachea and human airway epithelium. Proc Natl Acad Sci U S A. 2009;106:12771–5.
2. Rawlins EL, Okubo T, Xue Y, Brass DM, Auten RL, Hasegawa H, et al. The role of Scgb1a1 + Clara cells in the long-term maintenance and repair of lung airway, but not alveolar, epithelium. Cell Stem Cell. 2009;4:525–34.
3. Xiao H, Li DX, Liu M. Knowledge translation: Airway epithelial cell migration and respiratory diseases. Cell Mol Life Sci. 2012;69:4149–62.
4. Plopper CG, Hyde DM. Epithelial Cells of the Bronchiole. In: Parent RA, editor. Comparative Biology of the Normal Lung. 2nd ed. Waltham: Academic Press; 2015. pp. 83–92.
5. Ghosh M, Ahmad S, White CW, Reynolds SD. Transplantation of Airway Epithelial Stem/Progenitor Cells: A Future for Cell-Based Therapy. Am J Respir Cell Mol Biol. 2017;56:1–10.
6. Toba H, Wang Y, Bai X, Zamel R, Cho HR, Liu H, et al. XB130 promotes bronchioalveolar stem cell and Club cell proliferation in airway epithelial repair and regeneration. Oncotarget. 2015;6:30803–17.
7. Rosen C, Shezen E, Aronovich A, Klionsky YZ, Yaakov Y, Assayag M, et al. Preconditioning allows engraftment of mouse and human embryonic lung cells, enabling lung repair in mice. Nat Med. 2015;21:869–79.
8. Wong AP, Dutly AE, Sacher A, Lee H, Hwang DM, Liu M, et al. Targeted cell replacement with bone marrow cells for airway epithelial regeneration. Am J Physiol Lung Cell Mol Physiol. 2007;293:L740–L52.
9. Park KS, Wells JM, Zorn AM, Wert SE, Laubach VE, Fernandez LG, et al. Transdifferentiation of ciliated cells during repair of the respiratory epithelium. Am J Respir Cell Mol Biol. 2006;34:151–7.
10. Giangreco A, Reynolds SD, Stripp BR. Terminal bronchioles harbor a unique airway stem cell population that localizes to the bronchoalveolar duct junction. Am J Pathol. 2002;161:173–82.
11. Verschoyle RD, Martin J, Dinsdale D. Selective inhibition and induction of CYP activity discriminates between the isoforms responsible for the activation of butylated hydroxytoluene and naphthalene in mouse lung. Xenobiotica. 1997;27:853–64.
12. Stripp BR, Maxson K, Mera R, Singh G. Plasticity of airway cell proliferation and gene expression after acute naphthalene injury. Am J Physiol. 1995;269:L791–9.

13. Plopper CG, Suverkropp C, Morin D, Nishio S, Buckpitt A. Relationship of cytochrome P-450 activity to Clara cell cytotoxicity. I. Histopathologic comparison of the respiratory tract of mice, rats and hamsters after parenteral administration of naphthalene. J Pharmacol Exp Ther. 1992;261:353–63.
14. Kim CF, Jackson EL, Woolfenden AE, Lawrence S, Babar I, Vogel S, et al. Identification of bronchioalveolar stem cells in normal lung and lung cancer. Cell. 2005;121:823–35.
15. Dovey JS, Zacharek SJ, Kim CF, Lees JA. Bmi1 is critical for lung tumorigenesis and bronchioalveolar stem cell expansion. Proc Natl Acad Sci U S A. 2008;105:11857–62.
16. Teisanu RM, Lagasse E, Whitesides JF, Stripp BR. Prospective isolation of bronchiolar stem cells based upon immunophenotypic and autofluorescence characteristics. Stem Cells. 2009;27:612–22.
17. Zacharek SJ, Fillmore CM, Lau AN, Gludish DW, Chou A, Ho JW, et al. Lung stem cell self-renewal relies on BMI1-dependent control of expression at imprinted loci. Cell Stem Cell. 2011;9:272–81.
18. Tropea KA, Leder E, Aslam M, Lau AN, Raiser DM, Lee JH, et al. Bronchioalveolar stem cells increase after mesenchymal stromal cell treatment in a mouse model of bronchopulmonary dysplasia. Am J Physiol Lung Cell Mol Physiol. 2012;302:L829–L37.
19. Sun R, Zhou Q, Ye X, Takahata T, Ishiguro A, Kijima H, et al. A change in the number of $CCSP^{pos}/SPC^{pos}$ cells in mouse lung during development, growth, and repair. Respir Investig. 2013;51:229–40.
20. Lee JH, Bhang DH, Beede A, Huang TL, Stripp BR, Bloch KD, et al. Lung stem cell differentiation in mice directed by endothelial cells via a BMP4-NFATc1-thrombospondin-1 axis. Cell. 2014;156:440–55.
21. Basil MC, Morrisey EE. BASC-ing in the glow: bronchioalveolar stem cells get their place in the lung. EMBO J. 2019;38:e102344.
22. Liu Q, Liu K, Cui G, Huang X, Yao S, Guo W, et al. Lung regeneration by multipotent stem cells residing at the bronchioalveolar-duct junction. Nat Genet. 2019;51:728–38.
23. Salwig I, Spitznagel B, Vazquez-Armendariz AI, Khalooghi K, Guenther S, Herold S, et al. Bronchioalveolar stem cells are a main source for regeneration of distal lung epithelia in vivo. EMBO J. 2019;38:e102099.
24. Liu K, Tang M, Liu Q, Han X, Jin H, Zhu H, et al. Bi-directional differentiation of single bronchioalveolar stem cells during lung repair. Cell Discov. 2020;6:1.
25. McQualter JL, Yuen K, Williams B, Bertoncello I. Evidence of an epithelial stem/progenitor cell hierarchy in the adult mouse lung. Proc Natl Acad Sci U S A. 2010;107:1414–9.
26. Driscoll B, Kikuchi A, Lau AN, Lee J, Reddy R, Jesudason E, et al. Isolation and characterization of distal lung progenitor cells. Methods in molecular biology. 2012;879:109–22.
27. Takahashi K, Yamanaka S. Induction of pluripotent stem cells from mouse embryonic and adult fibroblast cultures by defined factors. Cell. 2006;126:663–76.
28. Momozane T, Fukui E, Funaki S, Fujii M, Kinehara Y, Ito E, et al. Efficient Differentiation of Mouse Induced Pluripotent Stem Cells into Alveolar Epithelium Type II with a BRD4 Inhibitor. Stem Cells Int.

2019;2019:1271682.

29. Pimton P, Lecht S, Stabler CT, Johannes G, Schulman ES, Lelkes PI. Hypoxia enhances differentiation of mouse embryonic stem cells into definitive endoderm and distal lung cells. Stem Cells Dev. 2015;24:663–76.
30. Katsirntaki K, Mauritz C, Olmer R, Schmeckebier S, Sgodda M, Puppe V, et al. Bronchoalveolar sublineage specification of pluripotent stem cells: effect of dexamethasone plus cAMP-elevating agents and keratinocyte growth factor. Tissue Eng Part A. 2015;21:669–82.
31. Fox E, Shojaie S, Wang J, Tseu I, Ackerley C, Bilodeau M, et al. Three-dimensional culture and FGF signaling drive differentiation of murine pluripotent cells to distal lung epithelial cells. Stem Cells Dev. 2015;24:21–35.
32. Zhou Q, Ye X, Sun R, Matsumoto Y, Moriyama M, Asano Y, et al. Differentiation of mouse induced pluripotent stem cells into alveolar epithelial cells in vitro for use in vivo. Stem cells translational medicine. 2014;3:675–85.
33. Sun H, Quan Y, Yan Q, Peng X, Mao Z, Wetsel RA, et al. Isolation and characterization of alveolar epithelial type II cells derived from mouse embryonic stem cells. Tissue Eng Part C Methods. 2014;20:464–72.
34. Otsuki K, Imaizumi M, Nomoto Y, Nomoto M, Wada I, Miyake M, et al. Effective embryoid body formation from induced pluripotent stem cells for regeneration of respiratory epithelium. Laryngoscope. 2014;124:E8–14.
35. Garreta E, Melo E, Navajas D, Farre R. Low oxygen tension enhances the generation of lung progenitor cells from mouse embryonic and induced pluripotent stem cells. Physiol Rep. 2014;2.
36. Schmeckebier S, Mauritz C, Katsirntaki K, Sgodda M, Puppe V, Duerr J, et al. Keratinocyte growth factor and dexamethasone plus elevated cAMP levels synergistically support pluripotent stem cell differentiation into alveolar epithelial type II cells. Tissue engineering Part A. 2013;19:938–51.
37. Ninomiya N, Michiue T, Asashima M, Kurisaki A. BMP signaling regulates the differentiation of mouse embryonic stem cells into lung epithelial cell lineages. In Vitro Cell Dev Biol Anim. 2013;49:230–7.
38. Alipio ZA, Jones N, Liao W, Yang J, Kulkarni S, Sree Kumar K, et al. Epithelial to mesenchymal transition (EMT) induced by bleomycin or TFG_{b1}/EGF in murine induced pluripotent stem cell-derived alveolar Type II-like cells. Differentiation. 2011;82:89–98.
39. Roszell B, Mondrinos MJ, Seaton A, Simons DM, Koutzaki SH, Fong GH, et al. Efficient derivation of alveolar type II cells from embryonic stem cells for in vivo application. Tissue Eng Part A. 2009;15:3351–65.
40. Rippon HJ, Polak JM, Qin M, Bishop AE. Derivation of distal lung epithelial progenitors from murine embryonic stem cells using a novel three-step differentiation protocol. Stem Cells. 2006;24:1389–98.
41. Ali NN, Edgar AJ, Samadikuchaksaraei A, Timson CM, Romanska HM, Polak JM, et al. Derivation of type II alveolar epithelial cells from murine embryonic stem cells. Tissue Eng. 2002;8:541–50.

42. Reynolds SD, Malkinson AM. Clara cell: Progenitor for the bronchiolar epithelium. Int J Biochem Cell Biol. 2010;42:1–4.
43. Winkler ME, Mauritz C, Groos S, Kispert A, Menke S, Hoffmann A, et al. Serum-free differentiation of murine embryonic stem cells into alveolar type II epithelial cells. Cloning Stem Cells. 2008;10:49–64.
44. Oliver JR, Kushwah R, Wu J, Cutz E, Yeger H, Waddell TK, et al. Gender differences in pulmonary regenerative response to naphthalene-induced bronchiolar epithelial cell injury. Cell Prolif. 2009;42:672–87.
45. Tan JL, Lau SN, Leaw B, Nguyen HPT, Salamonsen LA, Saad MI, et al. Amnion Epithelial Cell-Derived Exosomes Restrict Lung Injury and Enhance Endogenous Lung Repair. Stem Cells Transl Med. 2018;7:180–96.
46. Volckaert T, Dill E, Campbell A, Tiozzo C, Majka S, Bellusci S, et al. Parabronchial smooth muscle constitutes an airway epithelial stem cell niche in the mouse lung after injury. J Clin Invest. 2011;121:4409–19.
47. Mandai M, Watanabe A, Kurimoto Y, Hirami Y, Morinaga C, Daimon T, et al. Autologous Induced Stem-Cell-Derived Retinal Cells for Macular Degeneration. N Engl J Med. 2017;376:1038–46.
48. Kawamura M, Miyagawa S, Miki K, Saito A, Fukushima S, Higuchi T, et al. Feasibility, safety, and therapeutic efficacy of human induced pluripotent stem cell-derived cardiomyocyte sheets in a porcine ischemic cardiomyopathy model. Circulation. 2012;126:29–37.
49. Petersen TH, Calle EA, Zhao L, Lee EJ, Gui L, Raredon MB, et al. Tissue-engineered lungs for in vivo implantation. Science. 2010;329:538–41.
50. Ott HC, Clippinger B, Conrad C, Schuetz C, Pomerantseva I, Ikonomou L, et al. Regeneration and orthotopic transplantation of a bioartificial lung. Nat Med. 2010;16:927–33.
51. Mitchell A, Wanczyk H, Jensen T, Finck C. Human induced pluripotent stem cells ameliorate hyperoxia-induced lung injury in a mouse model. Am J Transl Res. 2020;12:292–307.
52. Shafa M, Ionescu LI, Vadivel A, Collins JJP, Xu L, Zhong S, et al. Human induced pluripotent stem cell-derived lung progenitor and alveolar epithelial cells attenuate hyperoxia-induced lung injury. Cytotherapy. 2018;20:108–25.
53. Kotton DN, Morrisey EE. Lung regeneration: mechanisms, applications and emerging stem cell populations. Nature medicine. 2014;20:822–32.
54. Soh BS, Zheng D, Li Yeo JS, Yang HH, Ng SY, Wong LH, et al. $CD166^{pos}$ subpopulation from differentiated human ES and iPS cells support repair of acute lung injury. Mol Ther. 2012;20:2335–46.
55. Weiss DJ, Bertoncello I, Borok Z, Kim C, Panoskaltsis-Mortari A, Reynolds S, et al. Stem cells and cell therapies in lung biology and lung diseases. Proc Am Thorac Soc. 2011;8:223–72.
56. Germano D, Blyszczuk P, Valaperti A, Kania G, Dirnhofer S, Landmesser U, et al. Prominin-1/$CD133^{+}$ lung epithelial progenitors protect from bleomycin-induced pulmonary fibrosis. Am J Respir Crit Care Med. 2009;179:939–49.

Figures

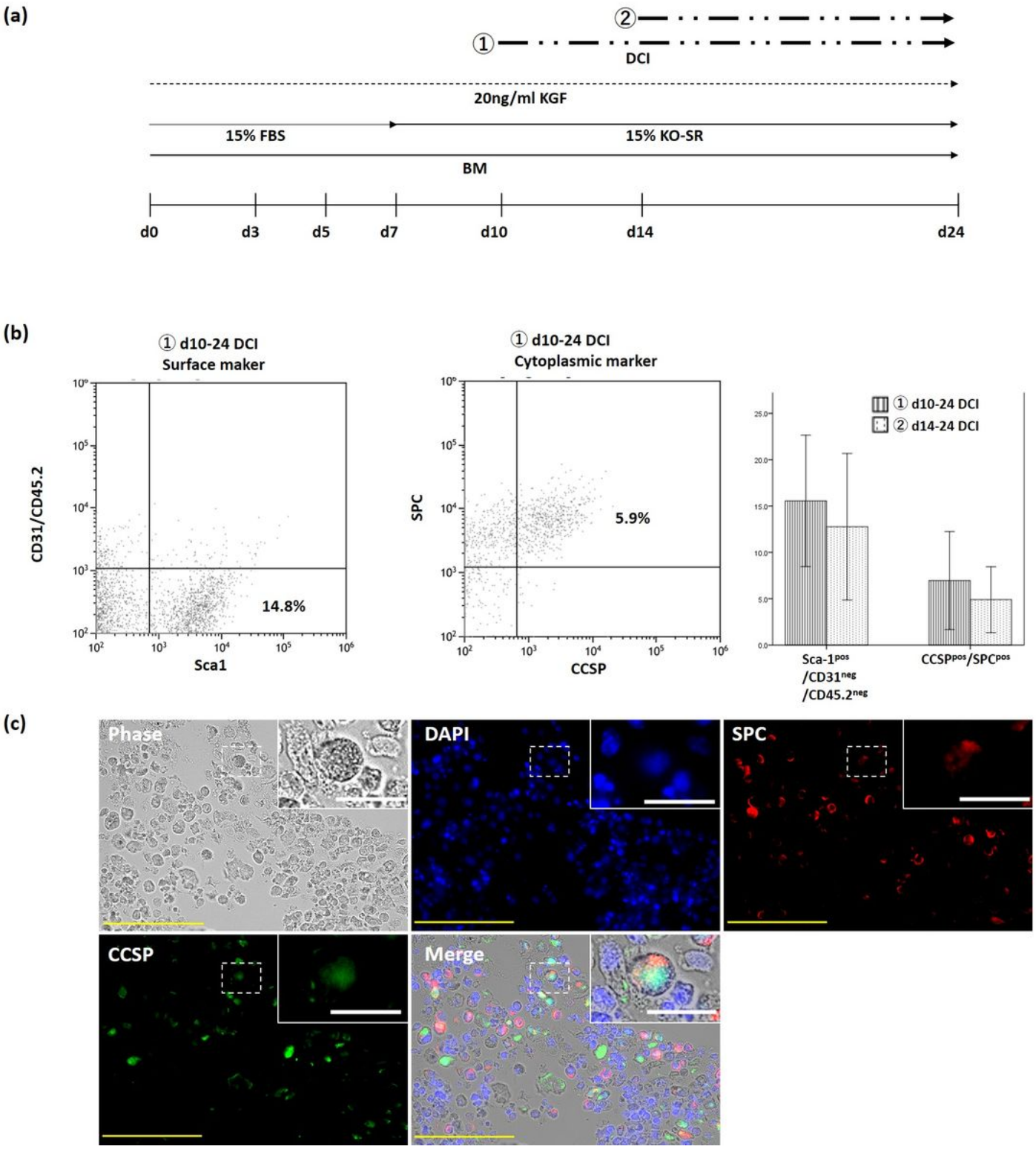

Figure 1

Differentiation of iPSCs into BASCs. a Schema of iPSC differentiation procedure: iPSCs were differentiated for 24 days through hanging-drop-based formation of embryoid bodies (EBs); the BM was supplemented from 0 to 24 d with 20 ng/mL keratinocyte growth factor (KGF) and DCI (□d10–d24 or

d14–d24). EBs were induced using the hanging-drop method for the first three days, and the obtained EBs were transferred at 3 d to super-low-adherent culture dishes and then at 5 d to adherent cultures dishes. Cells were cultured until 24 d in the medium. b Flow cytometry analysis for BASC identification. Comparison of protocols d10–d24 DCI and d14–d24 DCI revealed that BASC differentiation efficiency did not differ significantly between the protocols (P > 0.05); data are shown as means ± SD. c Immunofluorescence labelling of iPSC-derived differentiated cells. Yellow scale bar = 100 μm; white scale bar = 20 μm. DCI: 10 nM dexamethasone plus 0.1 mM 8-bromoadenosine 3´5´-cyclic monophosphate sodium salt and 0.1 mM 3-isobutyl-1-methylxanthine; iPSCs: induced pluripotent stem cells; BASCs: bronchioalveolar stem cells.

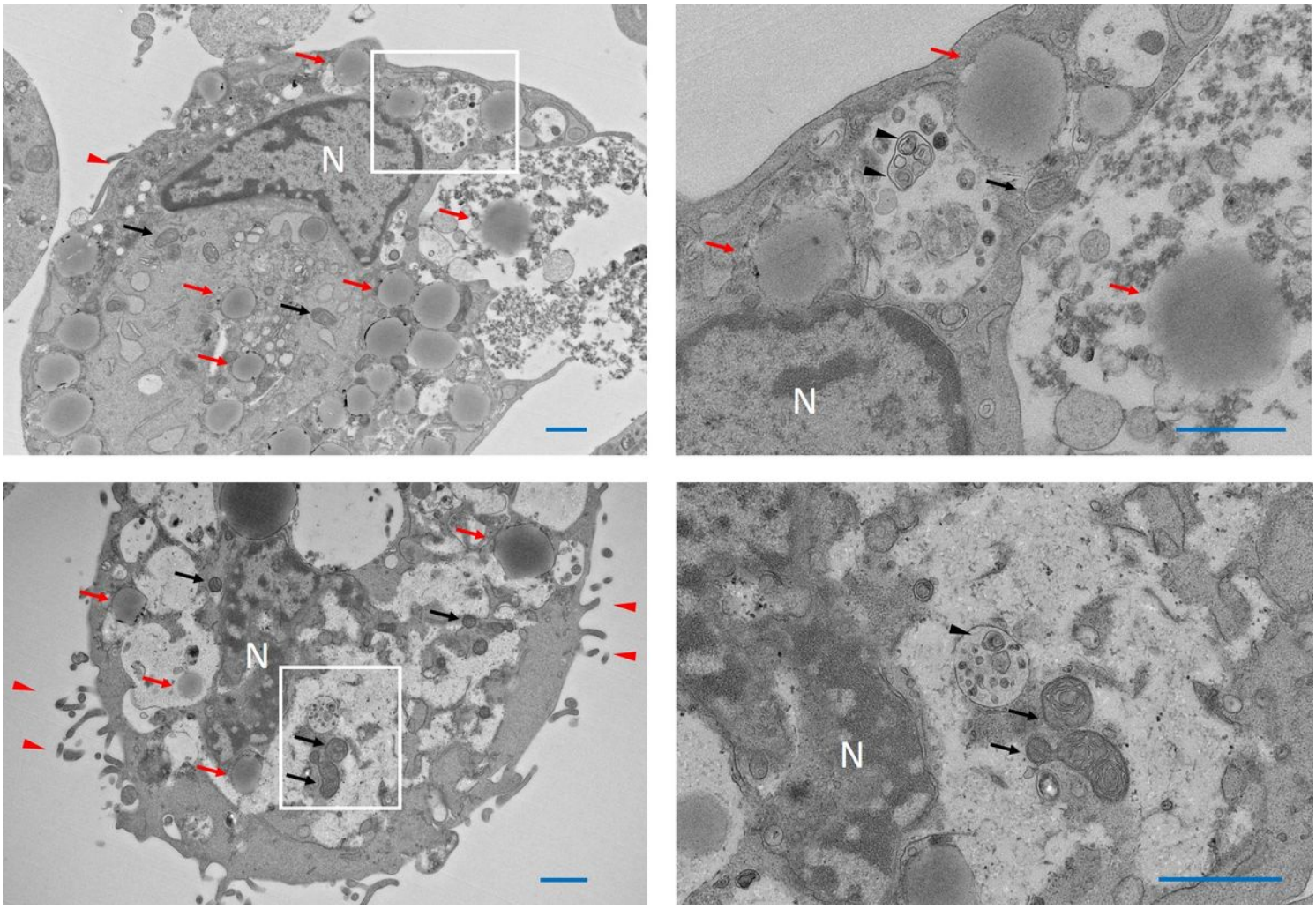

Figure 2

Transmission electron micrographs of iPSC-derived BASCs. A single BASC is shown containing microvilli (red arrowhead), immature lamellar body-like structures (black arrowhead), and secretory granules (red arrow); black arrow: mitochondria. Scale bar = 1 μm. iPSCs: induced pluripotent stem cells; BASCs, bronchioalveolar stem cells

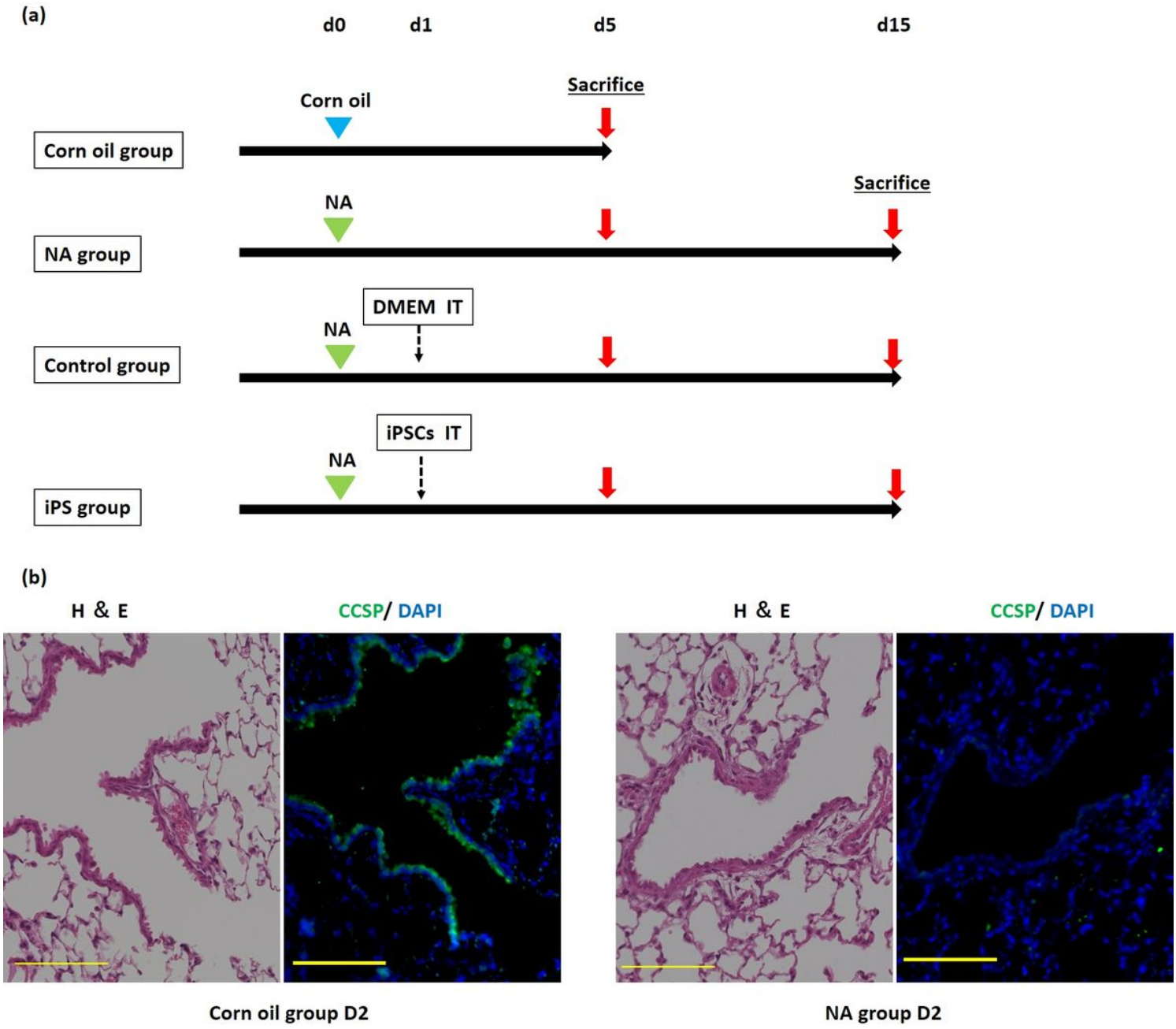

Figure 3

Establishment of mouse distal airway injury model. a Schematic showing experimental design. Corn oil or naphthalene was injected intraperitoneally into mice at 0 d. At 1 d, DMEM and differentiated iPSCs were intratracheally administered in the control and iPS groups, respectively. Mice were sacrificed at 5 d and 15 d (n = 4–6 at each time point). b Preparation of naphthalene-treatment model. Corn oil and NA groups are shown from the second day after treatment. In the NA group, CCSP-positive club cells (green) were completely detached. NA: naphthalene treatment; iPSCs: induced pluripotent stem cells; IT: intratracheal injection; BW: body weight; H&E: hematoxylin and eosin; CCSP: club-cell secretory protein; DAPI: 4′,6-diamidino-2-phenylindole dihydrochloride; ANOVA, analysis of variance. c Change in body weight from baseline. Data represent means ± SD from separate experiments. *P < 0.05 iPS group vs

control group; **P < 0.01 iPS group vs control and NA groups; one-way ANOVA followed by Tukey's multiple-comparison test

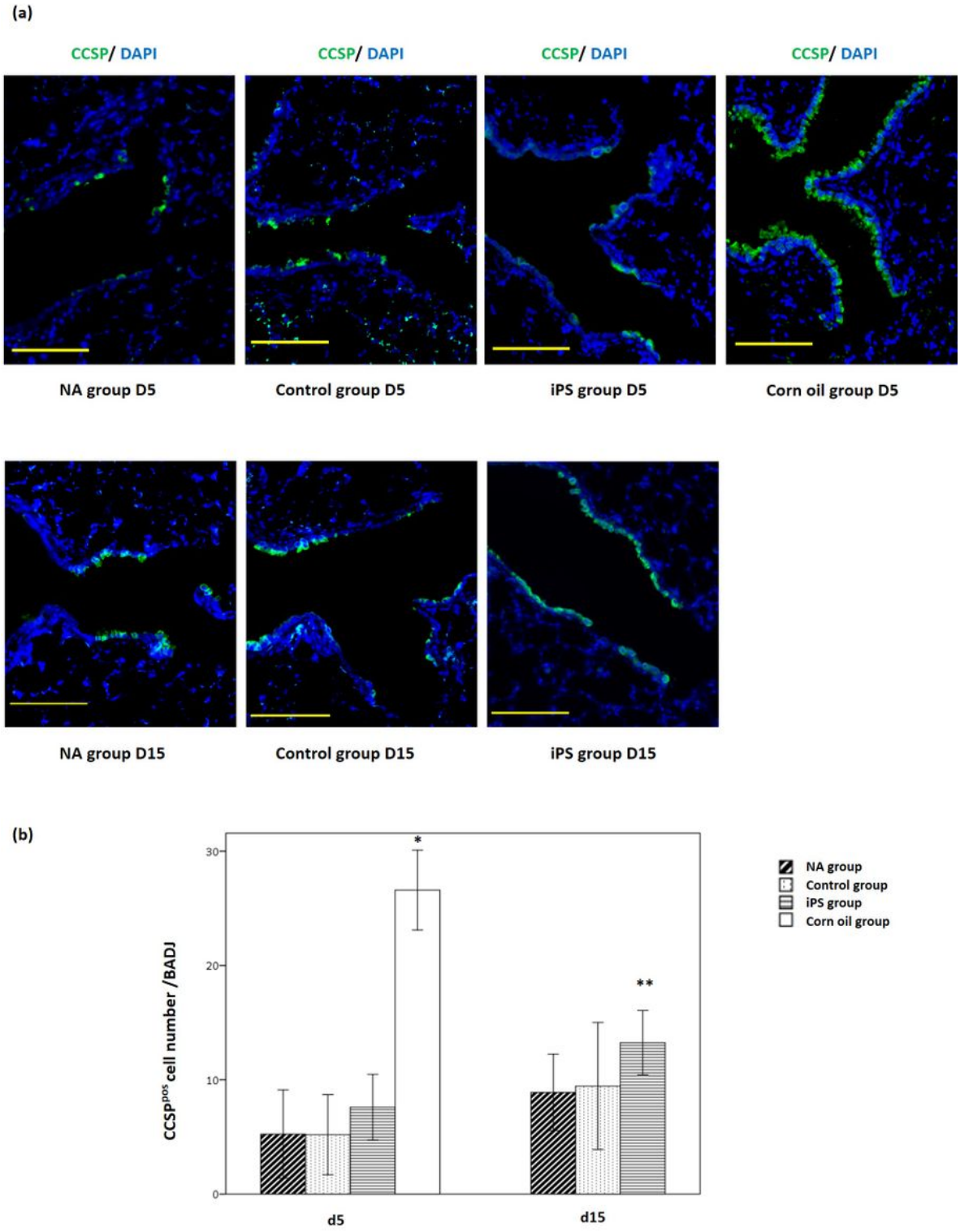

Figure 4

Quantification of CCSP-positive club cells at BADJs at 5 d and 15 d after naphthalene treatment. a Immunofluorescence labelling of club cell marker CCSP (green) in each group. Nuclei were counterstained with DAPI (blue). Scale bar = 100 μm. b Comparison of numbers of CCSP-positive cells at BADJs. Data

are shown as means ± SD. *P < 0.01, **P < 0.05 vs all other groups; one-way ANOVA followed by Tukey's multiple-comparison test. CCSP: club-cell secretory protein; BADJs: bronchioalveolar-duct junctions; DAPI: 4´,6-diamidino-2-phenylindole dihydrochloride

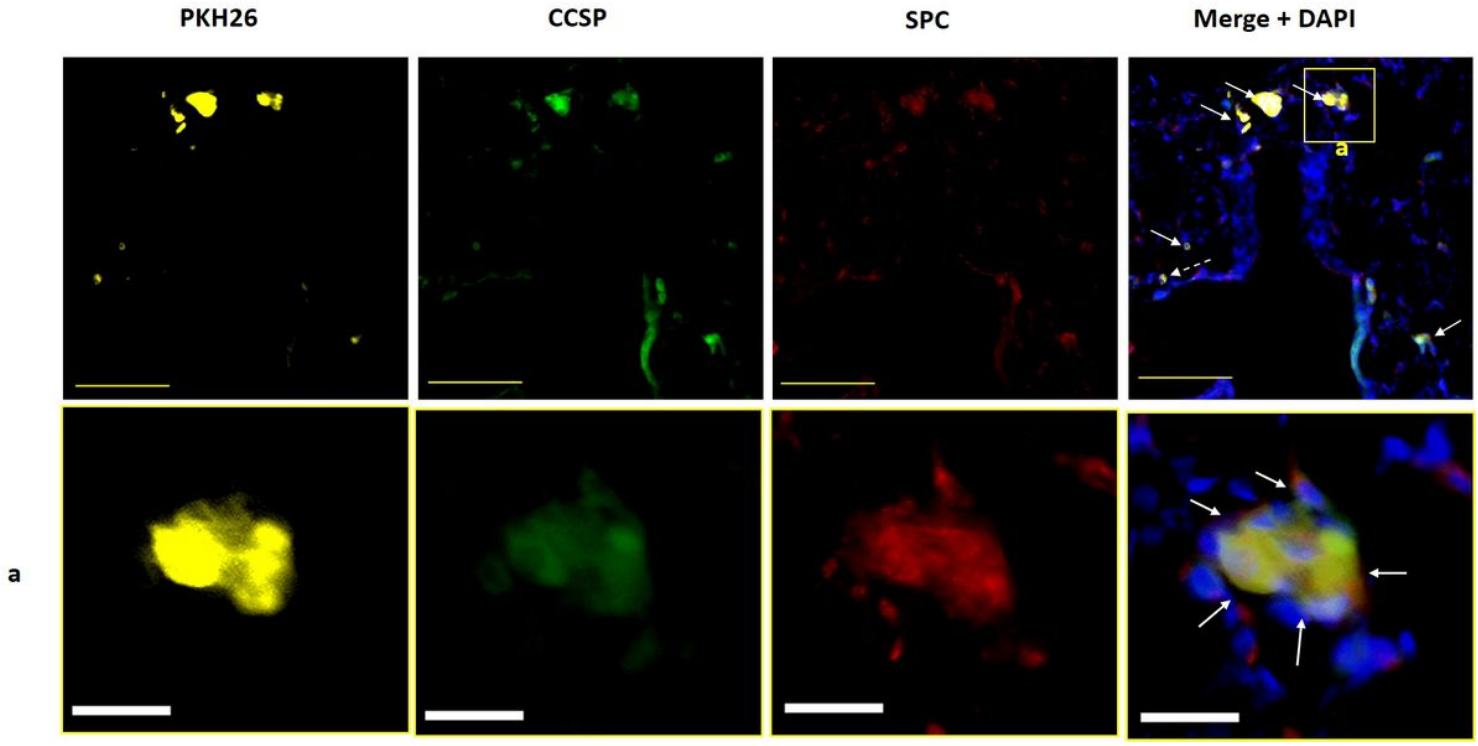

Figure 5

Immunofluorescence labelling of CCSP and SPC in mouse frozen lung sections at 5 d after intratracheal transplantation of differentiated iPSCs. Differentiated iPSCs were labelled with PKH26 cell tracker (yellow). Nuclei were counterstained with DAPI (blue). PKH26-positive, CCSP-positive (green), and SPC-positive (red) cells (PKHpos/CCSPpos/SPCpos cells, white arrow), which are BASCs, were present around BADJs. PKHpos/CCSPneg/SPCneg cells (white dotted arrow) were also detected. Bottom panels: magnified view of area a in top panel. PKHpos/CCSPpos/SPCpos cells formed clumps. Yellow scale bar = 100 μm; white scale bar = 20 μm. CCSP: club-cell secretory protein; SPC: surfactant protein C; iPSCs: induced pluripotent stem cells; BADJs: bronchioalveolar-duct junctions; DAPI: 4´,6-diamidino-2-phenylindole dihydrochloride

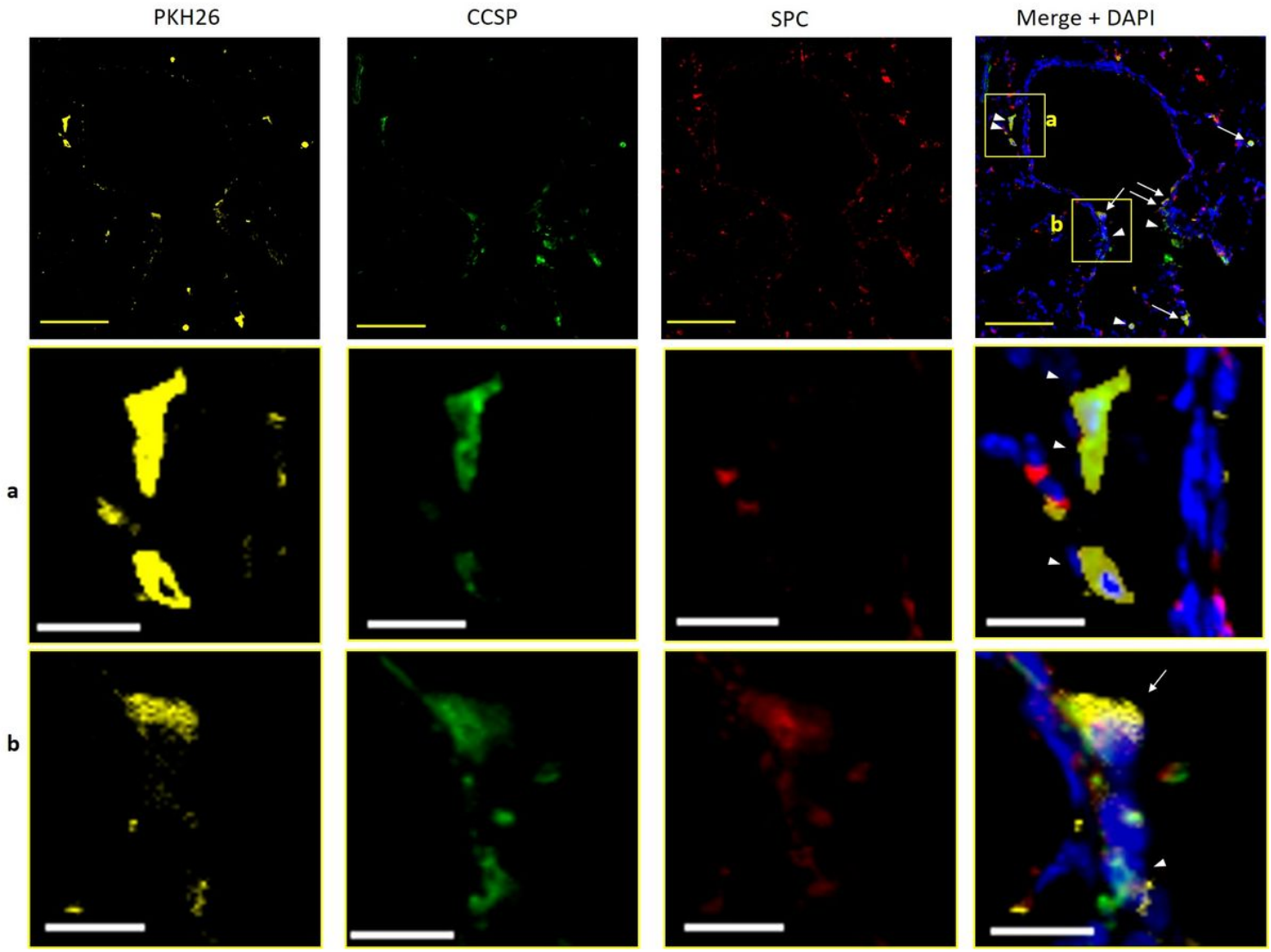

Figure 6

Immunofluorescence labelling of CCSP and SPC in mouse frozen lung sections at 15 d after intratracheal transplantation of differentiated iPSCs. Differentiated iPSCs were labelled with PKH26 cell tracker (yellow). Nuclei were counterstained with DAPI (blue). PKH26-positive, CCSP-positive (green), and SPC-positive (red) cells (PKHpos/CCSPpos/SPCpos cells, white arrow), which are BASCs, were found as part of the epithelium of the BADJ. PKHpos/CCSPpos/SPCneg cells (white arrowhead), which are club cells, were scattered. Middle and bottom panels: magnified view of areas a and b in top panel, respectively. CCSP: club-cell secretory protein; SPC: surfactant protein C; iPSCs: induced pluripotent stem cells; BADJs: bronchioalveolar-duct junctions; DAPI:

Supplementary Files

This is a list of supplementary files associated with this preprint. Click to download.

- Additionalfile1.docx